Journal of the Korean Physical Society, Vol. 60, No. 7, April 2012, pp. 1087∼1091

Unipolar Resistance Switching Characteristics in a Thick ZnO/Cu/ZnO Multilayer Structure

Tran LE and Hoang Cao Son TRAN
Faculty of Physics and Engineering Physics, University of Science, Vietnam National University - HoChiMinh City, Vietnam

Van Hieu LE and Tuan TRAN
Faculty of Materials Science, University of Science, Vietnam National University - HoChiMinh City, Vietnam

Cao Vinh TRAN
Laboratory of Advanced Materials, University of Science, Vietnam National University - HoChiMinh City, Vietnam

Thanh Tan VO
University of Technical Education, HoChiMinh City, Vietnam

Mau Chien DANG
Laboratory of Nanotechnology, Vietnam National University - HoChiMinh City, Vietnam

Sang Sub KIM
School of Materials Science and Engineering, Inha University, Incheon 402-751, Korea

Jaichan LEE
School of Advanced Materials Science and Engineering, Sungkyunkwan University, Suwon 440-746, Korea

Bach Thang PHAN*
Faculty of Materials Science and Laboratory of Advanced Materials, University of Science, Vietnam National University - HoChiMinh City, Vietnam

(Received 7 November 2011, in final form 2 February 2012)

The resistance switching mechanism and the electrical conduction of thick Cu/ZnO/Cu/ZnO/Cu structures were investigated for various ZnO thicknesses (40, 80, 160, and 320 nm) when the thickness of the middle Cu layer was 2 nm. The ZnO films had a microstructure with columnar grains normal to the substrate. The switching voltages (V_{SET} and V_{RESET}) varied with the thickness of the ZnO layer. A symmetric electrode structure exhibited a unipolar resistance switching. The electrical transport of both high-resistance state (HRS) and low-resistance state (LRS) was Ohmic conduction, and the resistance switching mechanism was driven by the formation and the rupture of Cu conducting paths.

PACS numbers: 77.80.Fm
Keywords: Resistance switching, Random access memory, Sputtering, ZnO
DOI: 10.3938/jkps.60.1087

I. INTRODUCTION

The resistance random access memory (ReRAM) has recently become a promising non-volatile memory due to its scalability, low power consumption, fast switching speed and nondestructive readouts [1–9]. The ReRAM devices consist of many different kinds of material systems. Therefore, many resistance mechanisms have been proposed. These mechanisms can be categorized into three types: electronic, thermal and ionic [2]. The ionic

*E-mail: pbthang@hcmus.edu.vn, pbthang@skku.edu

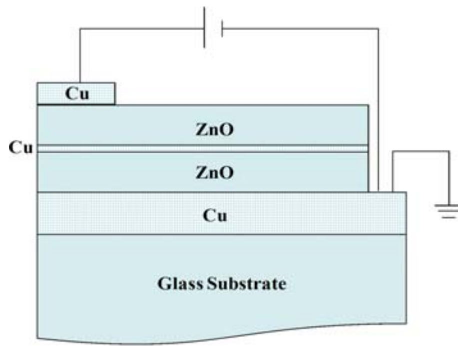

Fig. 1. (Color online) Schematic diagram of the Cu/ZnO/Cu/ZnO/Cu structure.

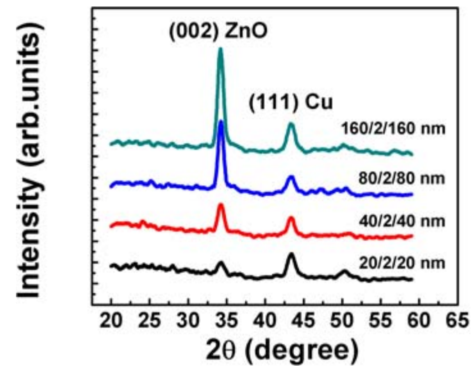

Fig. 2. (Color online) XRD patterns of the Cu/ZnO/Cu/ZnO/Cu structure for various ZnO thicknesses.

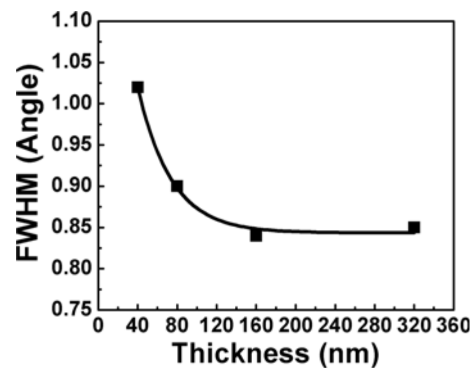

Fig. 3. FWHM values of the (002) diffraction peaks from ZnO films with different thicknesses.

resistive switching mechanism is driven by the transport and the electrochemical reactions of cations (Ag^+ or Cu^{n+}) or anions (O^{n-}) in structures with the presence of an active electrode (Ag, Au or Cu) and an inert electrode (Pt, W...) [2,8,9]. Typical bipolar switching is one of the prerequisite characteristic of the ionic mechanism. Yang *et al.* observed nanoscale Ag bridges penetrating through the ZnO layer in the Ag/ZnO:Mn/Pt structure and thus, attributed the bipolar resistive switching mechanism to redox-reaction-mediated formation and rupture of Ag bridges [8]. The bipolar switching transition from carrier trapping/detrapping (electronic mechanism) to electrochemical metallization (ionic mechanism) in the Cu/ZnO/Cu/ZnO/Pt structure is found to be mainly related to the altered status of Cu atoms [9]. In this study, we investigated the resistance switching in the symmetric Cu/ZnO/Cu/ZnO/Cu structure for the following reasons: (1) Replacing expensive Pt electrode with Cu electrode is needed for feasible production of a ReRAM because Cu material is currently used in integrated circuit technology. (2) In Cu-doped oxide - based ReRAM systems [9–13], the thickness of the oxide layer is just a few tens of nm. We aimed to identify the resistance switching mechanism in a thicker ZnO layer of hundreds of nm to investigate the variations in the switching voltages (V_{SET} and V_{RESET}).

II. EXPERIMENTS AND DISCUSSION

A proposed schematic of the Cu/ZnO/Cu/ZnO/Cu structure is shown in Fig. 1. The Cu/ZnO/Cu/ZnO/Cu structure was fabricated from metallic Cu and ceramic ZnO targets by using the dc sputtering technique at room temperature. All deposition processes were carried out in an Ar gas ambient at pressures of 1.6×10^{-3} Torr and 2.4×10^{-3} Torr for the Cu layers and the ZnO layers, respectively. Metallic Cu layers, 120-nm and 80-nm-thick, were deposited as bottom and top electrodes at deposition powers of 36 W and 16.8 W, respectively. The ZnO/Cu/ZnO trilayer was prepared as follows: two ZnO layers of the same thickness (20 nm, 40 nm, 80 nm, and 160 nm) were deposited at a deposition power of 38 W. Between the two ZnO deposition processes, a Cu midlayer of 2 nm was sandwiched at a deposition power of 36 W. During the deposition of top the Cu layer, a mask was used for top electrode patterning. The thickness of these thin films were determined by using a quartz crystal microbalance during the deposition.

The crystalline phases and microstructures of the thin films were characterized in the θ-2θ mode by using a D8 Advance (Bruker) X-ray diffractometer (XRD) with Cu Kα radiation ($\lambda = 0.154$ nm) and field-emission scanning electron microscopy (FESEM). The chemical state of the Cu in the structure was characterized by using X-ray photoelectron spectroscopy (XPS). Current-voltage (I-V) measurements were carried out using a Keithley 2400 source meter and probe station. During the electrical measurement, a positive sweep voltage was applied to the Cu top electrode while the Cu bottom electrode was grounded.

Figure 2 shows the XRD patterns of the Cu/ZnO/Cu/ZnO/Cu structures with various ZnO thicknesses. From the XRD patterns, the crystal orientation is in the direction of the (002) plane for all structures. However, the degree of crystalline ordering varies with the ZnO thickness. The higher peak intensity of the thicker structure indicates that the thicker structures have better crys-

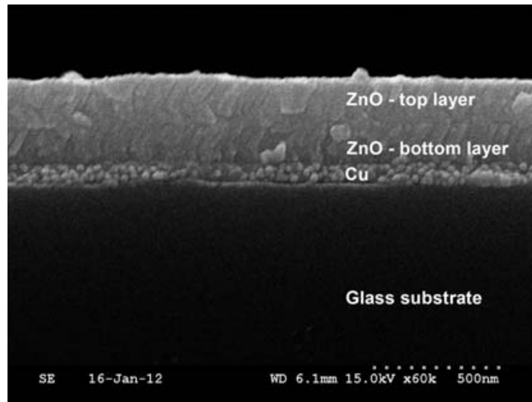

Fig. 4. Cross-sectional FESEM image of the 160/2/160 nm structure.

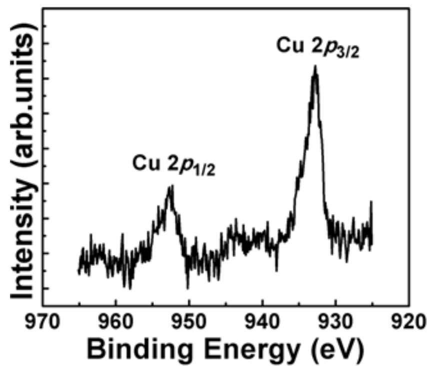

Fig. 5. Cu 2p core-level XPS spectrum the of 160/2/160 nm structure.

tallinity as deposited at room temperature. The reason for the improved crystallinity in the thicker structure can originate from the misfit strain between the ZnO film and the Cu bottom electrode. Figure 3 shows the full width at half maximum (FWHM) values of the (002) diffraction from ZnO films with various thicknesses. The films with a thickness of 20/2/20 nm show the largest FWHM because of the large misfit strain between the film and the Cu layer. As the film thickness increases, the FWHM values decreases. This result is attributed to the relaxation of the misfit strain with the formation of misfit dislocation in the films. Therefore, as the film thickness increases, the misfit strain decreases, resulting in better crystallinity.

The cross-sectional FESEM images of the 160/2/160 nm structure is shown in Fig. 4. The FESEM image reveals that the ZnO films have a microstructure of columnar grains. The columnar-grained structure is apparently related to the preferential growth of the basal plane of the ZnO material, leading to the formation of a highly (002)-oriented texture, which is observed in the XRD result. Since the Cu layer is so thin (2 nm), we cannot observe this layer clearly. However, there is a discontinuity growth at the middle region between the two ZnO layers due to the Cu layer. The chemical state of Cu in

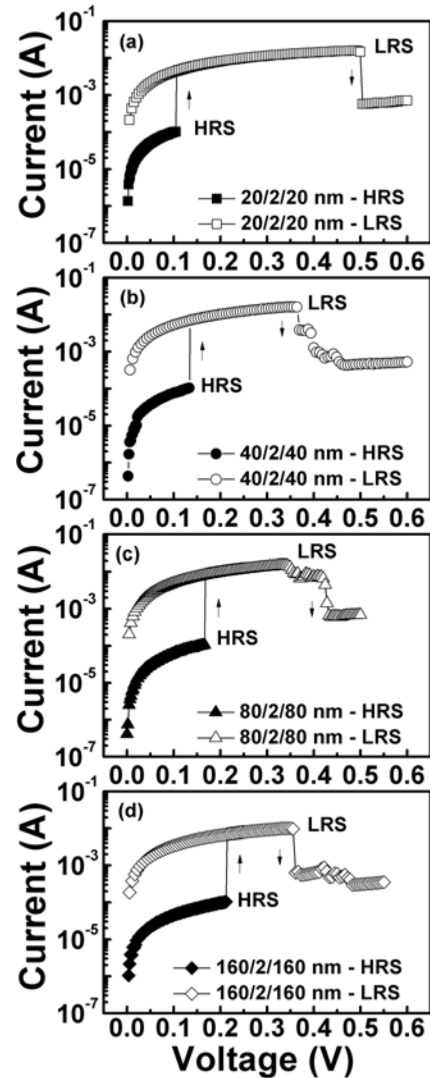

Fig. 6. Typical unipolar resistance switching characteristics of the Cu/ZnO/Cu/ZnO/Cu structures.

the 160/2/160 nm structure is shown in Fig. 5. The Cu $2p_{3/2}$ and Cu $2p_{1/2}$ peaks are located at binding energies of 932.8 and 952.7 eV, respectively. These peaks reveal a +2 state of Cu [14].

Figure 6 shows the typical I-V characteristics of the ReRAMs based on Cu/ZnO/Cu/ZnO/Cu structures. The initial state of the as-prepared structures is the high-resistance state (HRS). To find the switching voltages, we applied a 0 to V_{max} sweep (V_{max} = 0.1 V, 0.15 V, 0.2 V...) to observe the switching processes. A compliance current was applied to prevent permanent structure breakdown in the set process. A sudden increase in current (a resistance decrease) from the HRS to the low-resistance state (LRS) is observed above 0.1 V. The LRS remains until the end of the sweep. The resistance switching can be induced without a forming process. LRS to HRS switching is induced above 0.35 V. During several sweeps, V_{SET} and V_{RESET} showed an insignif-

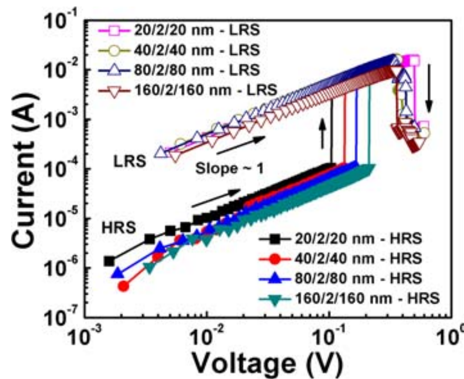

Fig. 7. (Color online) The log-log scale curves of the typical unipolar resistance switching characteristics in the HRS and the LRS.

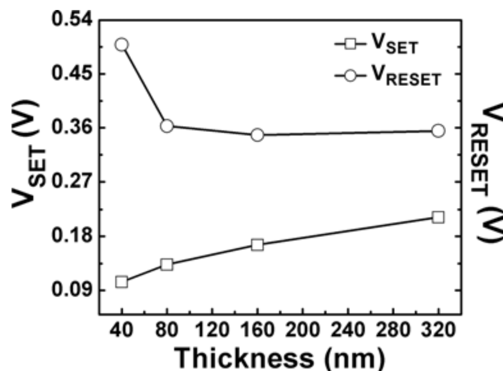

Fig. 8. Variations of V_{SET} and V_{RESET} with the ZnO thickness.

icant variation, with V_{SET} always being smaller than V_{RESET}. The lack of overlap between V_{SET} and V_{RESET} requires reliable device operation. The resistance switching follows a unipolar-type switching.

In order to understand the resistance switching behavior in these structures, we examined the transport characteristics. The leakage current of the HRS of ReRAM-based structures generally follows a nonlinear I-V dependence. However, as shown in Fig. 7, the leakage currents of both the HRS and the LRS of all the proposed structures show a linear dependence on voltage before switching. Because of this, such leakage mechanisms as space-charge-limited conduction, Schottky emission, and Poole-Frenkel emission were ruled out [15,16]. The leakage mechanisms of the HRS and the LRS obey Ohm's law, which gives clues to relate the physical origin of the resistive switching of these structures with the filament model [2,7]. However, we believe that the transports of carriers in both these states differ somewhat from each other.

The values of V_{SET} and V_{RESET} vary with the ZnO thickness, as shown in Fig. 6 and Fig. 8. The 20/2/20-nm-thick structure with the lowest crystallinity has the smallest V_{SET} and the largest V_{RESET} (Fig. 6(a)), while the 160/2/160-nm-thick structure with a higher degree of crystalline ordering shows the largest V_{SET} and the smaller V_{RESET} (Fig. 6(d)), what means that the V_{SET} value increases as the thickness of ZnO increases. As found above, the V_{SET} depends on the degree of crystalline ordering because a structure with low crystallinity has many empty spaces for forming the conductive paths easily. Therefore, the lower the crystallinity, the easier and stronger conductive paths will be formed (low V_{SET}). Consequently, the stronger the conductive paths formed, the harder it would be for the conductive paths to be ruptured (large V_{RESET}). In the thicker structures, higher voltages are required to form the conductive paths because the thick structures exhibit a highly (002) textured orientation with sharper peak and higher intensity and have a microstructure of columnar grains normal to the substrate, resulting a long-length, small-sized conductive paths. The high V_{SET} might only influence the length, not the size of the conductive paths. As a result, the V_{RESET} is significantly reduced in the 40/2/40-nm-thick structure compared to the 20/2/20-nm-thick structure, thus showing a lower dependence for the thicker structures.

In comparison, Yang *et al.* suggested that the associated electrical conductions of the HRS and the LRS in the carrier trapping/detrapping switching mechanism are space charge limited conduction (SCLC). In the electrochemical-redox-controlled switching mechanism, the HRS follows SCLC and the LRS obeys Ohm's law [9]. The two differences in the resistance switching behavior and transport conduction between our proposed structures and Yang's structures are as follows: our proposed structures depict unipolar switching, not bipolar switching, and Ohmic conduction of the HRS. Therefore, the Cu midlayer in our proposed structures might serve as a metallic bridge for electron hopping.

As argued above, the columnar grain structures make it easy for metallic defects to diffuse under the electric field through oxide layer. Since these hopping sites are close enough, conductive paths form and result in the LRS transition. Therefore, the transport conduction of the HRS obeys Ohm's law as follows: the electrons hop between metallic defects along with an alignment of metallic defects; consequently, the conductive paths of the metallic defects reach the electrodes when the voltage reaches V_{SET}. In the LRS, currents flow through the conductive paths, which also can be described by using Ohm's law. Since the switching is unipolar, the Joule-controlled LRS-to-HRS transition may be involved. This study has shown that resistance switching is caused by the formation and the rupture of the Cu conducting paths.

In order to give clear supporting data for the role of Cu conducting paths, we prepared the single layer structure glass/Cu/ZnO/Cu and Si/SiO_2/Ti/Pt/ZnO/Cu with a 160-nm-thick ZnO layer. We obtained unipolar resistance switching only in the glass/Cu/ZnO/Cu structure, not in the Si/SiO_2/Ti/Pt/ZnO/Cu structure. The electrical conduction of both the LRS and the HRS

in the glass/Cu/ZnO/Cu structure showed a linear I-V dependence, which is the same as in the glass/Cu/ ZnO/Cu/ZnO/Cu structure. On the other hand, the Cu/ZnO/Cu/ZnO structure without the top Cu electrode gives the same electrical conduction and resistance switching mechanism as the Cu/ZnO/Cu/ZnO/Cu structure. These results exclude the Cu ions originating from the top Cu electrode. In addition, the top Cu electrode exposed to the atmosphere ambient can be oxidized into Cu_xO, which can degrade the conductivity of the top electrode. However, we found that the I-V characteristics and the resistance switching mechanism did not vary with exposure time. Some Cu ions were induced from the bottom Cu electrode and the Cu midlayer during the deposition and then diffused into the ZnO matrix. Under the positive stress on the top electrode, the Cu ions diffuse to the bottom electrode and become Cu atoms there. As a result, the Cu conducting paths grow and approach the top interface, leading to HRS-to-LRS switching.

The intriguing point in this research is the values of V_{SET} and V_{RESET}; $V_{SET} < V_{RESET}$. This results is opposite to that in the Cu/ZnO/Cu/ZnO/Pt structure [9], but is the same as obtained in structures recently reported by Lee *et al.* and Linn *et al.* [17,18]. In Refs. 17 and 18, the switching behavior is induced in an anti-serially-connected memory structure. In comparison, we prepared a single Cu/ZnO/Cu structure. The single structure also exhibited the same switching behavior, in which the V_{SET} was smaller than the V_{RESET}. Additional experiments are underway in order to explain the above intriguing results.

III. CONCLUSION

In conclusion, we investigated the resistance switching mechanism and the electrical conduction of thick Cu/ZnO/Cu/ZnO/Cu structures. The ZnO films had a microstructure with columnar grains normal to the substrate. The chemical state of Cu in the structures was +2. The crystallinity of the ZnO layer depended on the ZnO thickness. As a result, the set voltage V_{SET} increased as the thickness of ZnO was increased while the reset voltage V_{RESET} decreased and became less dependent on the thickness for thicker ZnO layers. Symmetric electrode structures exhibited unipolar resistance switching. The electrical transport of both the HRS and the LRS followed an Ohmic conduction. The resistance switching mechanism was driven by the formation and the rupture of Cu conducting paths.

ACKNOWLEDGMENTS

This work was supported by National Foundation of Science and Technology Development of Vietnam (NAFOSTED - 103.99-2010.12), by the Vietnam National University - HoChiMinh city (B2011-18-26), and by the Basic Science Research Program through the National Research Foundation of Korea (2009-0092809).

REFERENCES

[1] C. Rossel, G. I. Meijer, D. Bremaud and D. Widmer, J. Appl. Phys. **90**, 2892 (2001).
[2] R. Waser and M. Anono, Nat. Mater. **6**, 833 (2007).
[3] B. T. Phan, T. Choi and J. Lee, J. Korean Phys. Soc. **51**, 664 (2007).
[4] B. T. Phan and J. Lee, Appl. Phys. Lett. **93**, 222906 (2008).
[5] B. T. Phan and J. Lee, Appl. Phys. Lett. **94**, 232102 (2009).
[6] B. T. Phan, N. C. Kim and J. Lee, J. Korean Phys. Soc. **54**, 873 (2009).
[7] D. B. Strukov, G. S. Snider, D. R. Stewart and R. S. Williams, Nature **453**, 80 (2008).
[8] Y. C. Yang, F. Pan, Q. Liu, M. Liu and F. Zeng, Nano Lett. **9**, 1636 (2009).
[9] Y. C. Yang, F. Pan, F. Zeng and M. Liu, J. Appl. Phys. **106**, 123705 (2009).
[10] C.-J. Li, S. Jou and W.-L. Chen, Jpn. J. Appl. Phys. **50**, 01BG08 (2011).
[11] S. Long, Q. Liu, H. Lv, Y. Li, Y. Wang, S. Zhang, W. Lian, K. Zhang, M. Wang, H. Xie and M. Liu, Appl. Phys. A **102**, 915 (2011).
[12] D. Lee, D. Seong, I. Jo, F. Xiang, R. Dong, S. Oh and H. Hwang, Appl. Phys. Lett. **90**, 122104 (2007).
[13] H. Choi, M. Pyun, T.-W. Kim, M. Hasan, R. Dong, J. Lee, J.-B. Park, J. Yoon, D. Seong, T. Lee and H. Hwang, IEEE Electron Device Lett. **30**, 302 (2009).
[14] M. Paschoalino, N. C. Guedes, W. Jardim, E. Mielczarski, J. A. Mielczar-ski, P. Bowen and J. Kiwi, J. Photochem. Photobiol., A **199**, 105 (2008).
[15] K. C. Kao and W. Huang, *Electrical Transport in Solids* (Pergamon, Oxford, UK, 1981).
[16] M. A. Lampert and P. Mark, *Current Injection in Solids* (Academic Press, NY, 1970).
[17] M.-J. Lee *et al.*, Nat. Mater. **10**, 625 (2011).
[18] E. Linn, R. Rosezin, C. Kügeler and R. Waser, Nat. Mater. **9**, 403 (2011).